ENGINEERING RESEARCH JOURNAL (ERJ)

Vol. 51, No. 2 April. 2022, pp.199-209

Journal Homepage: http://erj.bu.edu.eg

Numerical assessment of laterally loaded Pile-Tunnel interaction

Nasser M. Saleha, Ahmad M. Adamb, Waleed A. Dawoodc

[a] *Professor of Geotechnical Engineering, Civil Engineering Dep. Shoubra faculty, Benha University*

[b] *Teaching Assistant of Geotechnical Engineering, Civil Engineering Dep. Shoubra faculty, Benha University*

[c] *Assistant Professor of Geotechnical Engineering, Civil Engineering Dep. Shoubra faculty, Benha University*

Abstract

Accurate simulation of Pile-Tunnel interaction is crucial for the prediction of tunneling induced forces on nearby piled foundation and pile loading induced loads on existing tunnel lining. Number of studies in the literature investigated tunneling effect on piles numerically, by centrifuge modeling or by field monitoring. However, the effect of piles on tunnels, especially laterally loaded ones, is not well understood. This paper describes the application of 3D finite element model (FEM) to predict pile loading, vertically and laterally, effect on a nearby existing tunnel. Back analysis of a case history of greenfield tunneling and building response using 3D FEM show good agreement between predicted and observed displacements. The FEM applicability to simulate Pile-Tunnel interaction problem is proved by back analysis of field case study. The results of parametric studies show that pile loading increase bending moment, axial compression force and induce new tension force on tunnel lining with different percentage depending on Pile-Tunnel configuration. An influence zone of Loaded pile effect on existing tunnel is identified by clearance of 2DT and HT/LP ratio of 1.25. However, lateral load effect is more significant through a clearance of DT and HT/LP ratio of 0.5. Lateral load on pile contributes by 50% of induced B.M, 17% of induced compression axial force, 2% of induced tension axial force on tunnel lining and 100% of lateral deformation. On the other hand, pile axial load causes about 95% of induced vertical deformation of tunnel lining.

Keywords : Piles, Tunnels, Finite element, Lateral load

1. Introduction

The induced settlement at greenfield ground surface due to tunneling can be monitored in field [1] and can be predicted by empirical methods [2,3], analytical solutions [4] or numerical methods [5]. Tunneling induced ground movement affects nearby structures, so Withers [1,6] reported field data monitoring greenfield surface settlement and building response. Number of studies were concerned to model the effect of tunneling on nearby structures. Burd H.[7] proposed three-dimensional finite element model to simulate interaction between tunnel and building and predict crack pattern in the building. Pickhaver [5] presented a numerical model of to predict damage to masonry building using an approach of surface beams to model the building. On the other hand, Pile-Tunnel interaction is an important field of research. Marshall [9] presented an analytical solution to predict the response of an existing pile to a new tunnel construction. Pile response to twin tunneling had been predicted using three dimensional numerical parametric studies [10]. The other point of view of Pile-Tunnel interaction is the effect of newly constructed piled-foundation structure on an existing tunnel. Tunnel deformation, extension, and contraction of tunnel diameter, due to adjacent loaded piles was predicted using numerical assessment method [11]. The effect of pile construction on an existing tunnel was found to be ignored within a clearance of 1.0D between bridge pile tip and tunnel lining [12]. This paper proposes a three-dimensional finite element model, using PLAXIS® 3D program, to predict the effect of laterally loaded pile on an existing tunnel which is a problem that had not been sufficiently reported in literature. The first part describes in detail the finite element model used in this study. The proposed model has been verified by back analysis of field greenfield tunnel case and building response case. The validation of the proposed model to be applied on Pile-Tunnel interaction cases has been evaluated against field data.

2. THREE-DIMESIONAL FINITE ELEMENT MODEL VERIFICATION

Back analysis of case studied has been conducted to verify the proposed model in predicting greenfield surface settlement and response of buildings due to tunneling. The computed settlements are compared to the observed field data. Jubilee line extension project (JLE) is located in east London. The project consists of 11 station and 15.5 Km of two tunnel excavated using Earth pressure balanced machines (EPB) [1]. Field data were monitored at three reference sites. Southwark Park reference site was used in this study to verify greenfield surface settlement induced by tunneling and Niagara court reference site to verify Neptun house response to tunneling. Fig.1 shows the locations of reference sites in JLE project.

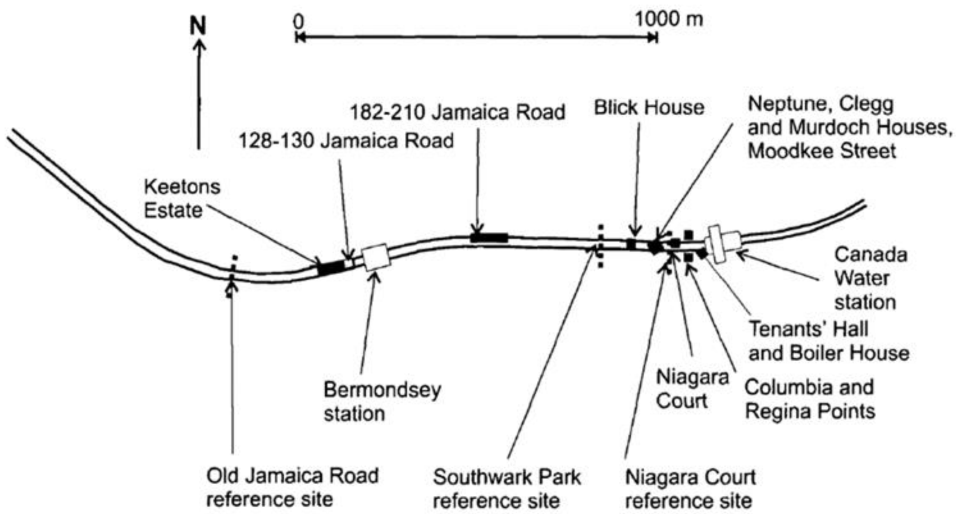

Fig 1. Locations of reference sites in Jubilee line extension project [1]

2.1. Ground condition and description of building

Soil layers in the reference sites are as follow; 2m of fill atop of about 4m of Thames gravel overlying various units of the Lambeth group extends to 20 to 25m. The Lambeth group lies on the top of Thanet bed layer to the top of chalk formation at a depth 40m [1].

Westbound tunnel centerline is located at a depth 21m below ground level with inner diameter 4.4m and lining of thickness 0.25m [1].

Neptun house is constructed of load bearing brick masonry in three-story height. The building is oriented with an angle of thirty with tunnel route. Building plan dimension are 40m by 8m [6]. Pickhaver [5] simplified the plan and section of footing of the building, this simplification is used for numerical modeling in this study.

2.2. Model geometry and boundary conditions

Model dimensions is recommended to be at least 4 to 5 times of tunnel diameter from tunnel centerline to the vertical model boundaries and 2 to 3 times of tunnel diameter to the bottom horizontal model boundary so that model boundaries wouldn't affect tunnel excavation induced deformations [13]. The studied case history was modeled using a geometry dimension of 60m in width, 100m in length and 40m in height as shown in Fig.2. and Fig.3. Symmetry about tunnel center line was exploited to reduce computational time. So only half the tunnel was modeled.

Vertical model boundaries parallel to the YZ-plane are fixed in X-direction and allowed to displace in Y- and Z-direction. On the other hand, vertical model boundaries parallel to the XZ-plane are fixed in Y-direction and free in Y- and Z-direction. The model bottom boundary is fixed in all directions and the top surface is free in all directions.

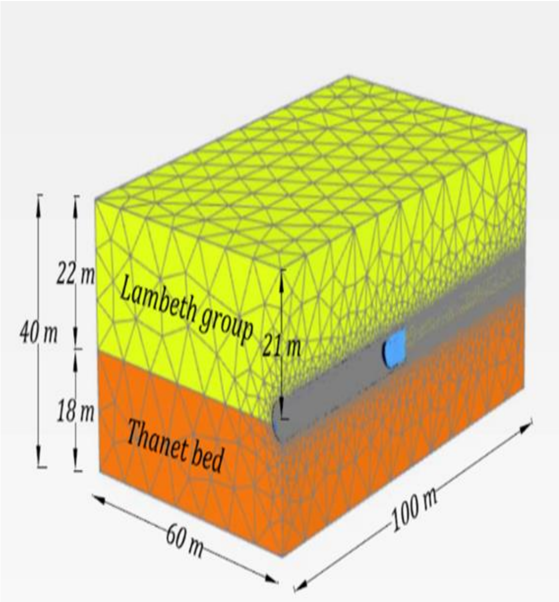

Fig 2. Southwark site greenfield model

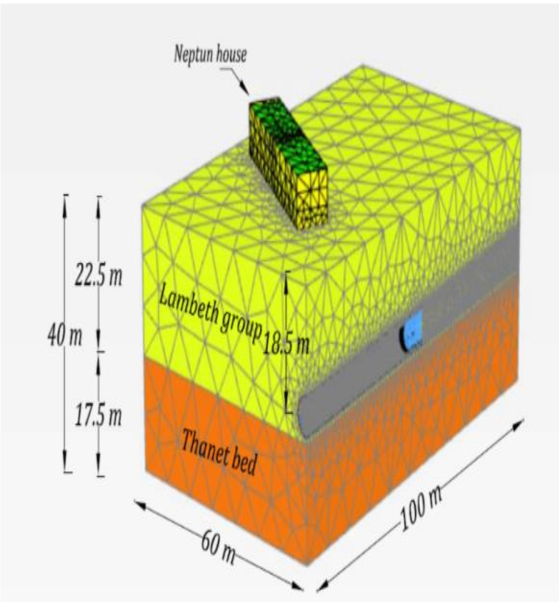

Fig 3. Tunnel under Neptun house model

2.3. Initial stress condition

Initial stress condition is defined by an initial vertical stress and initial horizontal stress which related to each other by the coefficient of lateral earth pressure K_o [14]. The initial stress condition is defined by a procedure called K_o procedure considering the loading history of soil, material model used, and soil parameter defined.

2.4. Soil, building parameters and material models

Mohr-coulomb material model was used to simulate soil behavior. Idealized soil profile given by Pickhaver [5] was used and shown in Table 1.

The footings of Neptun house were modeled ,on the same mesh geometry but with small differences in soil depths and tunnel center line depth, by linear-elastic concrete plate with thickness 0.43*m* and young's modulus of 20*GPa* with the simplified layout in Fig.4 given by Pickhaver [5], walls were modeled with the same layout by a linear elastic brick plate with thickness 0.225*m* and young's modulus of 3.5*GPa* and the slabs were modeled by a linear elastic concrete plate with thickness 0.25*m* and young's modulus of 20*GPa*. Table.2 summarizes modeling parameters of Neptun house.

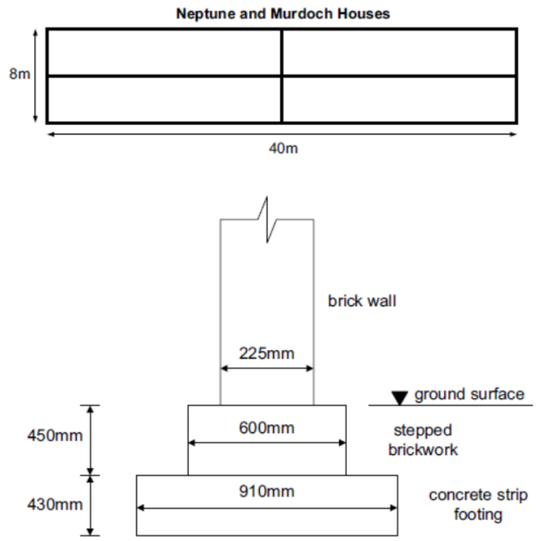

Fig 4. Simplified foundation detail of Neptun house

TABLE 1. Idealized soil profile for PLAXIS® 3D finite element model. After Pickhaver [5].

Layer	Lambeth group	Thanet bed
Material model	Mohr-Coulomb	Mohr-Coulomb
Depth (*m*)	22	18
γ (KN/m^3)	20	22
C_u (*KPa*)	40	210
E (*MPa*)	60	30
υ	0.495	0.49

TABLE 2. Neptun house modeling parameters

Element	Footing	Walls	Slabs
Material model	Linear elastic	Linear elastic	Linear elastic
Thickness (*m*)	0.43	0.225	0.25
γ (KN/m^3)	25	8	25
E (*GPa*)	20	3.5	20

2.5. Phased excavation of tunnel

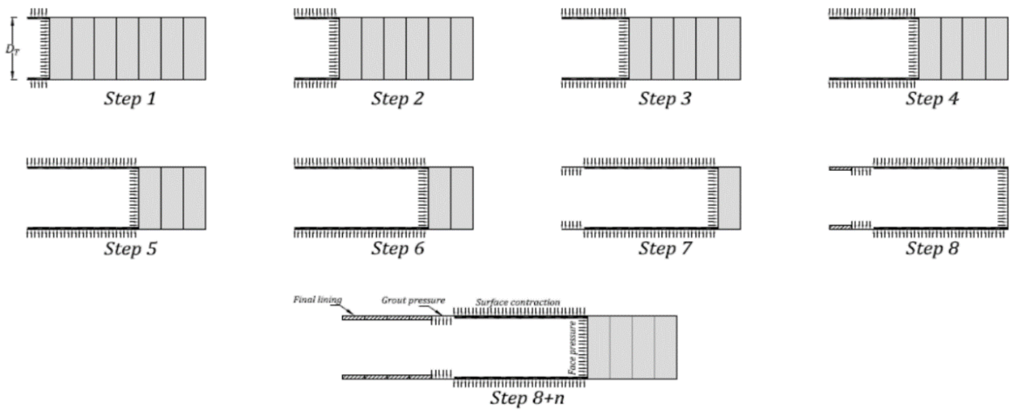

Fig 5. Tunnel advancement steps applied in the current study.

Installation procedure of Earth Pressure Balanced Tunnel Boring Machine (EPB-TBM), applied in the current study, is called "Phased excavation". Starting from initial stress state, all excavation steps are identical, except for its location, which will be shifted by a distance equal the TBM slice length, Fig.5 summarizes the excavation steps. Excavation is simulated be removing the soil elements inside the tunnel slice. Within the same step a perpendicular load distributed on the surface of the soil ring, immediately after the TBM tail ,is applied to simulate the grout pressure, and a ring of new lining elements is switched on to support the slice before. In each excavation step, the TBM shield is simulated by an elastic shell and the face pressure is modeled by surface distributed load on the excavation face with vertical increment with depth to have the same trapezoidal distribution as active soil pressure. The volume loss is simulated by applying a surface contraction to the TBM shell. Fig.6 presents a preview of tunnel excavation steps.
Westbound tunnel centerline is located at a depth 21 m below ground level with inner diameter 4.4 m and lining of thickness 0.25 m. Tunnel face pressure used in the model was 410 KN/m3 increasing with depth by 22 KN/m3

TABLE 3. Tunnel modeling parameters

	EPBM TBM	Tunnel lining
Material model	Linear elastic	Linear elastic
Thickness (*m*)	0.17	0.25
γ (KN/m^3)	247	27
E (*GPa*)	200	31
υ	0.1	0.1

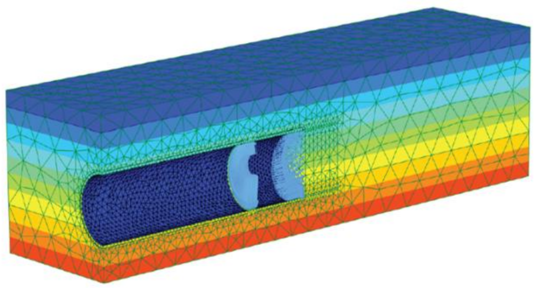

Fig 6. Preview of tunnel advancement in PLAXIS 3D program [15].

2.6. Results discussion

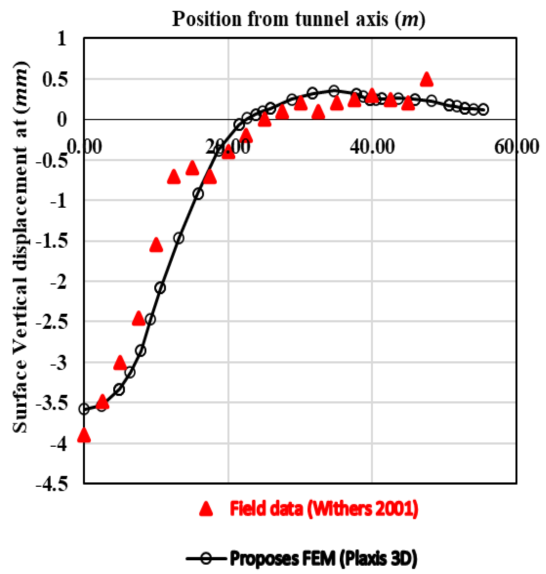

Fig 7. Southwark site surface settlement

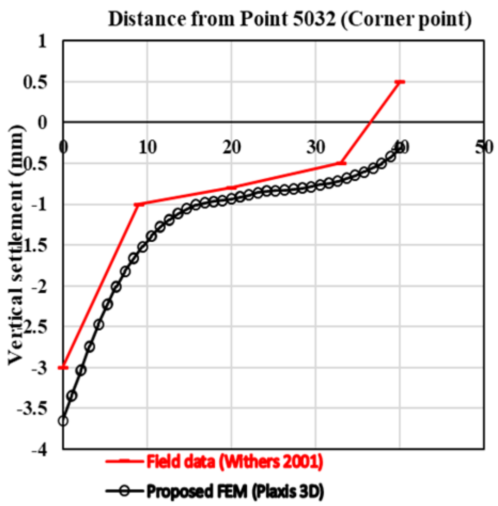

Fig 8. Neptun house response to tunneling

Results computed from the proposed FEM was compared to reported field data by Withers [1,6]. Fig.7 shows greenfield settlement for Southwark reference site due to tunneling of westbound tunnel. Maximum monitored settlement at field was 3.9mm and the predicted FEM maximum settlement was 3.59mm. The difference was +0.21m, then the error in the FEM was +7%. Results shown in Fig.8 presents the response of Neptun house for tunneling. Maximum monitored building settlement was 3mm while predicted FEM maximum building settlement was 3.64mm. The different was 0.64mm which produces an error of 21%. For both greenfield settlement and building response, predicted FEM results shows a good agreement with monitored field data.

3. VALIDATION OF FEM FOR PILE-TUNNEL INTERACTION ANALYSIS

The proposed model described in section.2 has been validated for Pile-Tunnel interaction analysis by back analysis of case study. MRT Northeast line, located in Singapore, is divided in construction to twelve contracts. The current study focuses on one of these contracts as a case study to validate pile response to tunneling in the proposed model. This case includes the construction of 2514m long twin tunnels and the construction of 1.9km long viaduct bridge supported on piled foundation. The viaduct bridge has a parallel alignment with the twin tunnels and located in between the tunnels [16].

3.1. Ground condition, Description of tunnel and piles

Tunnel and viaduct bridge piles are constructed through a completely weathered soil (Residual soil). The residual soil is classified as Grade VI (of the Bukit Timah Granite) according to the British code of practice (BS5930, 1981) [17] classified it as a G4 material [16]. Soil layers are defined by SPT-N value as shown in Fig.9.

Twin tunnels, namely southbound tunnel, and northbound tunnel, excavated with EBPM at a depth 21m. Both tunnels have an inner diameter 6m and located close to viaduct bridge piles i.e., 1.6m clear distance between tunnel and pile foundation. Pile foundation consist of a group of four bored piles of 1.2m diameter and 62m depth. In this case, the most of piles are installed before tunnels were excavated. Fig.9 shows the configuration of piles and tunnels.

3.2. PLAXIS® 3D finite element model

Soil was modeled using a geometry dimension of 60m in width, 100m in length and 60m in height Fig.10. This study focuses on pile response to construction of southbound tunnel (S.B) only, so symmetry about tunnel center line was exploited to reduce computational time and only half the tunnel was modeled. Mohr-coulomb material model was used to simulate soil behavior. Soil parameters, presented in Table.4, were derived by the correlations given by Zhang et al. [18] and Krank [19] due to lack of information about residual soils actual characteristic.

TABLE 4. Soil profile for PLAXIS® 3D finite element model.

Layer	Thickness (*m*)	γ (*KN/m*^{3})	Cu (*KPa*)	E (*MPa*)
G4 material (N = 0~15)	15	20	70	130
G4 material (N = 15~30)	25	20	125	280
G4 material (N = 30~50)	9	20	140	450
G3 material (N = 50~100)	11	20	225	500

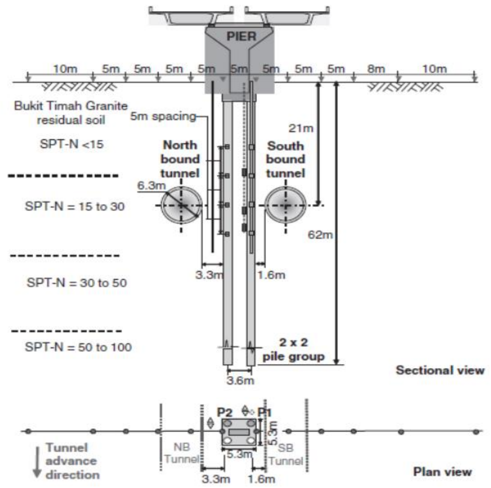

Fig 9. Typical bridge-tunnels configuration [16]

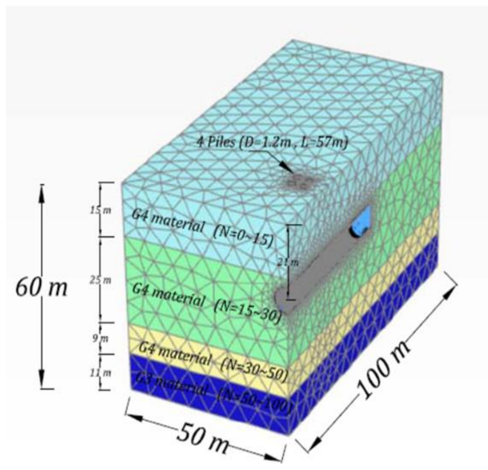

Fig 10. S.B Tunnel model geometry

Tunnel with inner radius 6m at depth 21m below ground level was excavated using EBP-TBM. Tunnel face pressure used in the model was 450 KN/m^3 increasing with depth by 20 KN/m^3. Tunnel modeling parameters presented in Table.3 was used.

On the other hand, there are two methods to model piles on PLAXIS® 3D program: embedded beam element and volume pile. Embedded beam is a structural element consists of beam element which interacts with the surrounding soil with special interface element. Pile-Soil interaction involves a skin resistance as well as foot resistance. The plastic behavior of soil in a volume around the embedded beam, of diameter equal to pile diameter, is excluded and assumed as elastic zone because the embedded beam element doesn't occupy any volume. While Volume pile is the technique modeling pile as a volume. At the pile location, soil corresponding to pile volume is removed and replaced by a concrete volume with its material definition. Pile-Soil interaction is simulated by an interface element around the perimeter of pile manually.

3.3. Results discussion

PLAXIS® 3D FEM predicted surface greenfield settlement induced by southbound tunnel against field monitored greenfield settlement is shown in Fig.11 Maximum tunnel induced surface settlement in field was 17.5*mm* while FEM predicted that of 17.93*mm*. overall settlement through has the same behavior in both field and FEM.

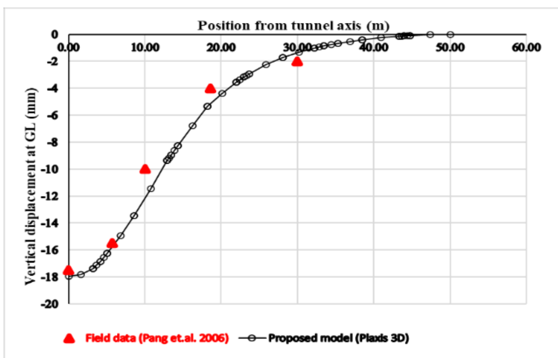

Fig 11. Greenfield surface settlement at MRT NEL site due to S.B tunnel excavation.

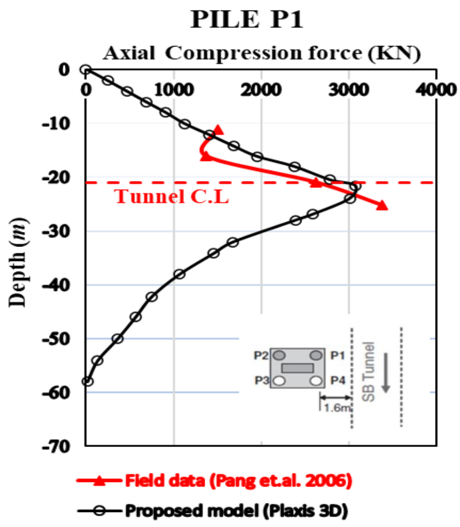

Fig 12. Pile P1 induced axial force

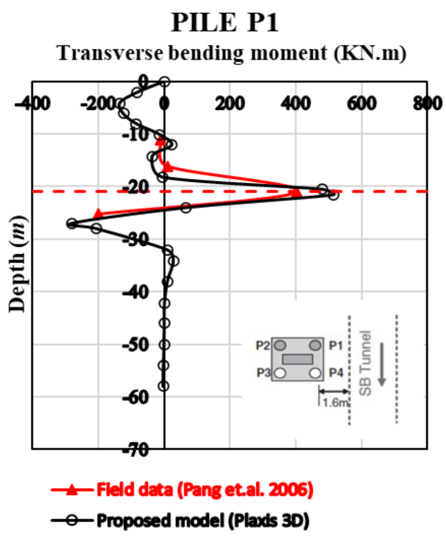

Fig 13. Pile P1 induced bending moment

Fig.12 and Fig.13 show induced forces in Pile P1 (The nearest pile of pile group to tunnel). Axial compression force shown in Fig.12 proves a good agreement between field data and computed forces in FEM. Maximum pile induced axial force was 3375*KN* in field and 3070*KN* in FEM. The difference between them was about 305*KN* which produces error of 10%. On the other hand, FEM predicted transverse bending moment in pile P1 shows excellent agreement with field monitored data as shown in Fig.13.
From results discussed above, it can be concluded that the proposed model shows an excellent applicability to simulate Pile-Tunnel interaction problems.

4. TUNNEL BEHAVIOR DUE TO LATERAL AND VERTICAL PILE LOADING IN DIFFERERNT CONGIGURATION

PLAXIS® 3D FEM, described in section.2 and validated for Pile-Tunnel interaction analysis in section.3, was adopted to investigate the effect of laterally and vertically loaded pile on a nearby tunnel. A set of parametric studies was made by varying Tunnel depth measured form pile foundation level to pile length ratio (H_T/L_P), clearance between pile and tunnel lining (*CL*), value, and direction of lateral load on pile and sandy soil type.

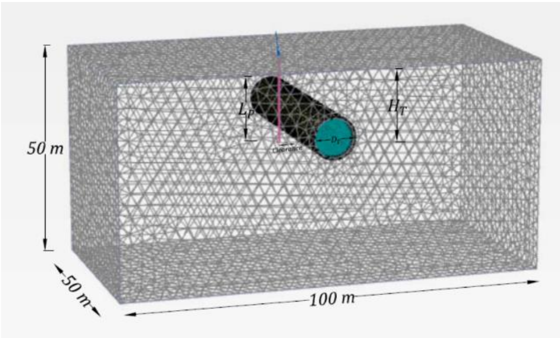

Fig 14. General 3D mesh geometry for parametric study

Greater Cairo underground metro tunnel configuration was taken. Tunnel external diameter of 9.15m, precast lining thickness of 0.4m and tunnel. internal diameter of 8.35m [20]. Besides, Pile length and diameter, assumed 20m,0.9m respectively, were constant in parametric studies to make it possible to assign constant vertical and lateral load. Fig.14 shows the general model geometry used for parametric study.
HT/LP of 0.25,0.5,0.75,1,1.25,2, clearance of 0.25DT, 0.50DT, DT, 2DT were investigated. These positions were arranged to cover the zones of influence of lateral and vertical load on pile. Fig.15 shows the configuration and tunnel positions investigated.
Furthermore, the effect of sandy soil type was studied through three cases: Loose sand, Medium dense sand, and Dense sand. Soil parameters were assumed according to Egyptian code of practice [21] as presented in Table.5. Moreover, lateral load effect was studied by varying its value and direction. Lateral load of 50%,75% and 100% of pile capacity was assigned in both positive and negative directions. Positive direction means that the load is in the direction of tunnel while negative direction is in the opposite.

TABLE 5. Soil Parameters for parametric study

Layer	Loose sand	M. Dense sand	Dense sand
Material model	Mohr-Coulomb	Mohr-Coulomb	Mohr-Coulomb
γ (KN/m^3)	18	19	20
φ	31	34	38
ψ	1	4	8
E (MPa)	17.5	50	123
υ	0.35	0.3	0.25

Tunnel lining forces, Bending Moment (B.M) and Normal Force (N.F), induced in tunnel lining were studied. Bending moments along tunnel lining due to greenfield soil stress (before pile loading) has negative and positive values while normal force acts as compression only. After Pile loading, positive, negative bending moment and compression normal force increase besides, tension normal force is produced. Fig.16 shows tunnel lining forces before and after pile loading

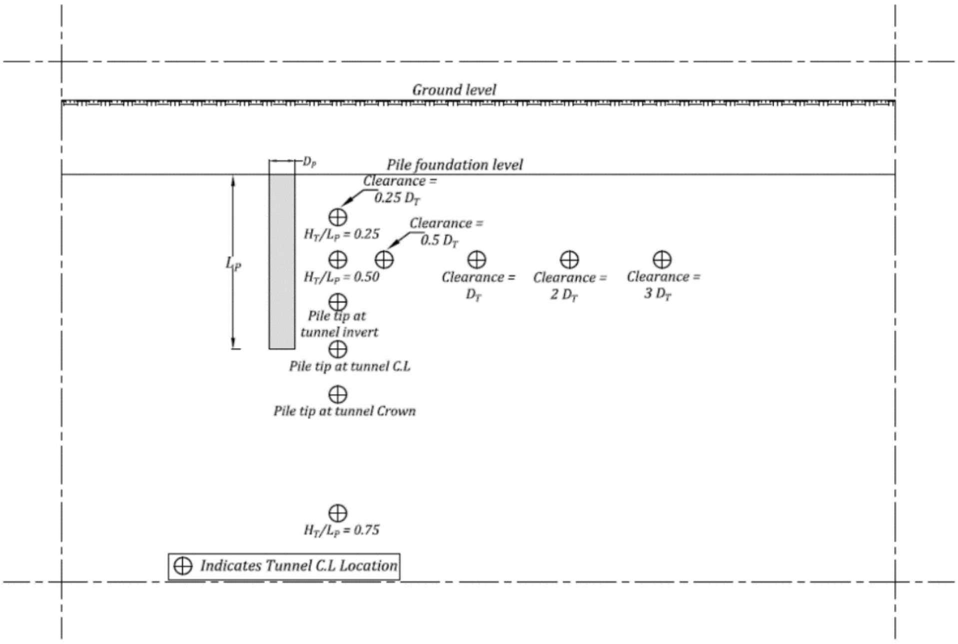

Fig 15. Configuration and tunnel positions investigated in the parametric studies.

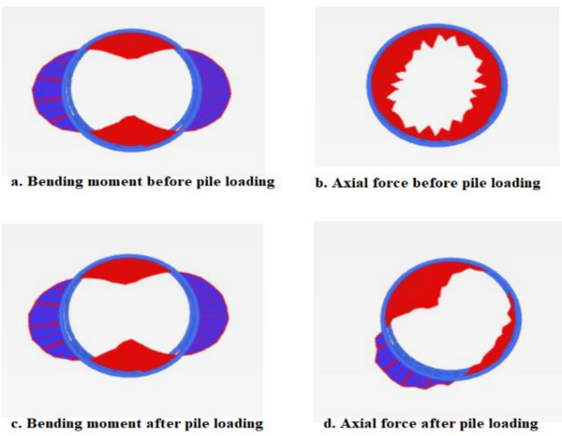

Fig 16. Tunnel lining forces before and after pile loading

4.1. Effect of HT/LP ratio

Results in Fig.17 and Fig.18 show that maximum induced B.M due to vertical load on pile occurs when pile tip is at tunnel crown while induced B.M due to lateral load on pile increases when tunnel get closer to pile head. On the other hand, induced axial force due to vertical and lateral load on pile decreases when H_T/L_P ratio increases. Induced deformations are shown in Fig.19, It's clear that vertical load has the most contribution in vertical deformation while lateral load has the most effect in lateral deformation.

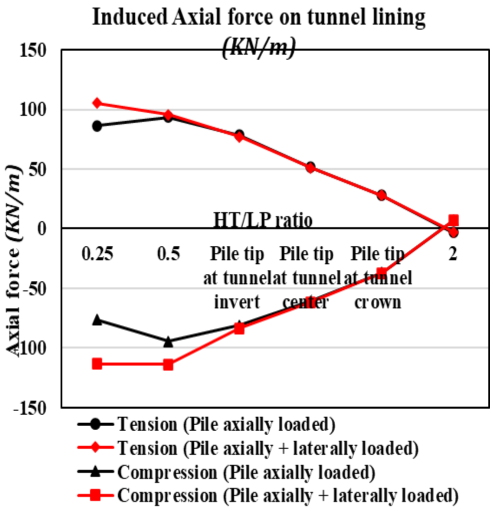

Fig 17. Lining induced B.M against H_T/L_P

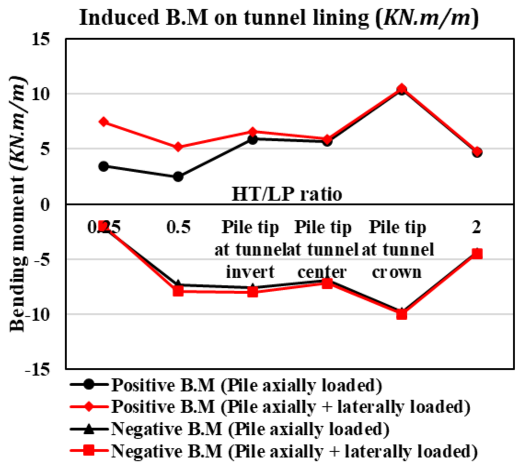

Fig 18. Lining induced A.F against H_T/L_P

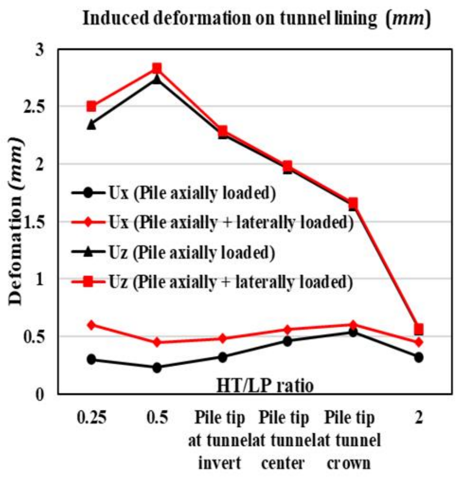

Fig 19. Lining induced deformations against H_T/L_P

4.2. Effect of Clearance

Fig.20 and Fig.21 show results for different clearances. Induced B.M and axial force due to vertical and lateral load on pile decrease while increasing clearance. The same for lining vertical and lateral deformations shown in Fig.22. When the clearance equal to or greater than $2D_T$, the effect of pile loading can be neglected, while effect of lateral load only can be neglected when the clearance equal to D_T or more.

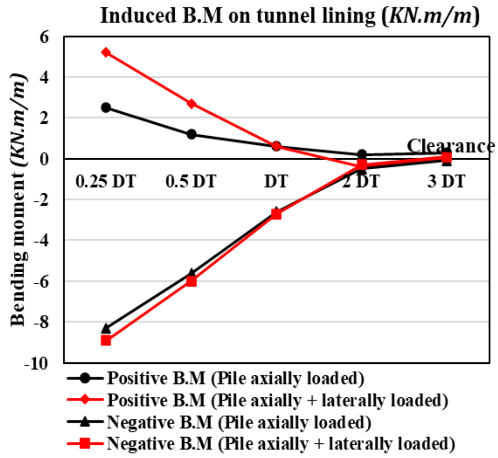

Fig 21. Lining induced A.F against *CL*

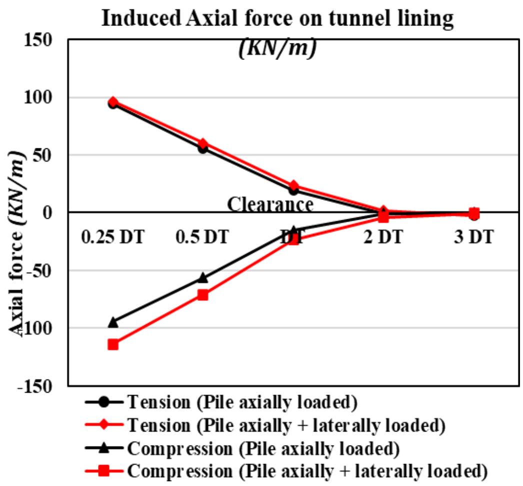

Fig 22. Lining induced deformations for different *CL*

4.3. Effect of Lateral load value and direction

Lateral load (L. Load) effect is well understood from results given in Fig.23 and Fig.24. When lateral load acts towards the tunnel, values of positive and negative B.M increase but for the opposite direction these values decrease. Furthermore, axial force has the same behavior as B.M. Fig.24 proves that the induced tension on tunnel lining is mainly due to vertical load on pile.

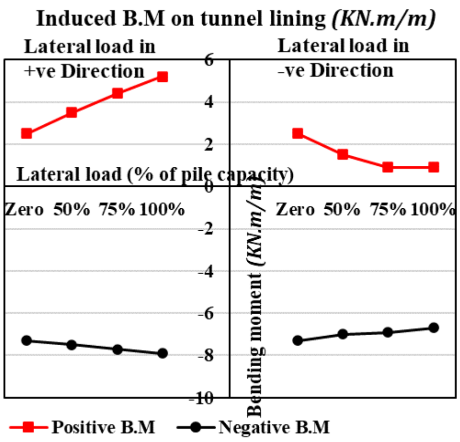

Fig 23. Lining induced B.M against L. Load

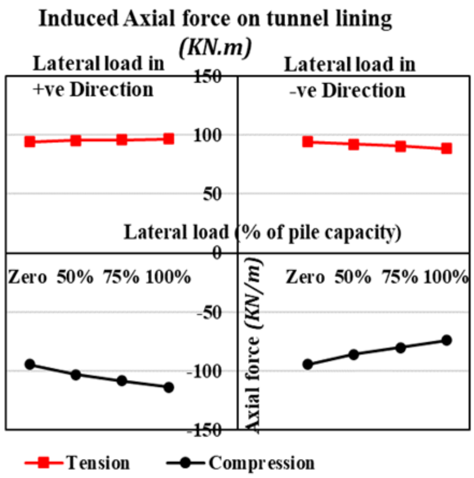

Fig 24. Lining induced A.F against L. Load

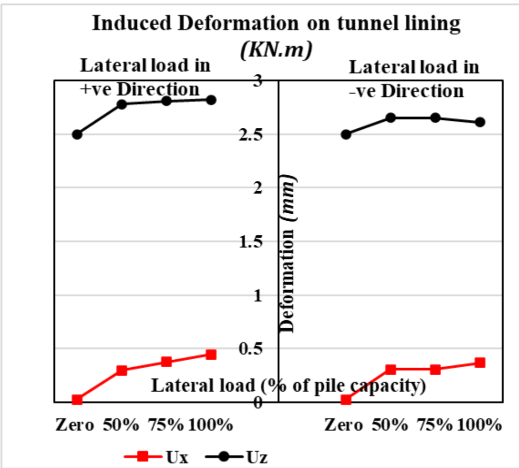

Fig 25. Lining induced deformations against L. Load

4.4. Effect of sandy soil type

It's clear that weaker the soil the more deformation it permits. Results in Fig.26, Fig.27 and Fig.28 prove this fact. The maximum effect of pile loading occurs in loose sand while medium dense sand gives medium effect, and the smallest effect occurs Dense sand. However, induced axial forces, both tension and compression, still significant in Dense sand.

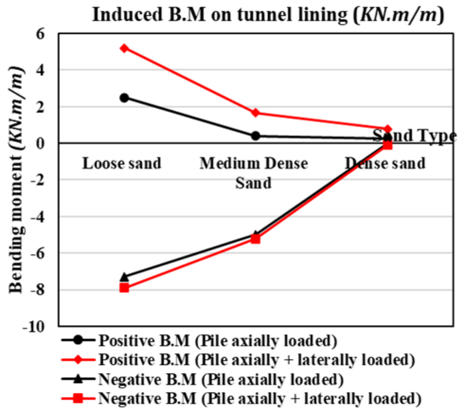

Fig 26. Lining induced B.M for against sand

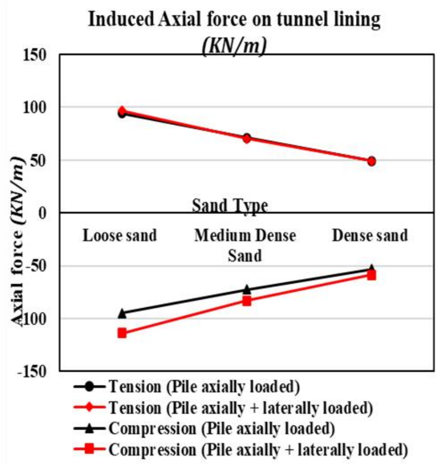

Fig 27. Lining induced A.F against sand

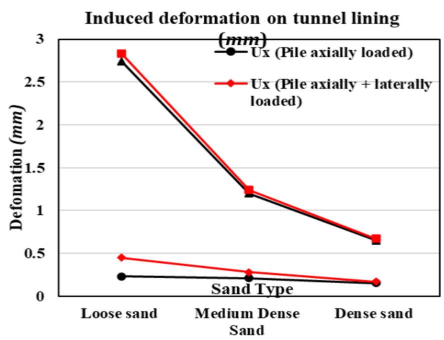

Fig 28. Lining induced deformations for different sand

5. CONCLOSION

This paper presents the application of three-dimensional finite element application to Pile-

Tunnel interaction problems. Based on computed results the following points can be concluded:

1- PLAXIS® 3D FEM indicates good agreement between predicted settlement and field data of greenfield tunneling and building response case histories.

2- Simulation of Pile-Tunnel interaction problems by the proposed FEM shows good suitability through back analysis of field case study.

3- Vertical and Lateral loads on piles cause increase of bending moment and axial force on the existing tunnel lining.

4- Induced bending moment on tunnel lining has a small value compared to that before pile loading while induced axial forces is the most important to compute because it has been transformed from compression to tension.

5- An influence zone of Loaded pile effect on existing tunnel is identified by clearance of 2DT and HT/LP ratio of 1.25 However, lateral load effect is more significant through a clearance of DT and HT/LP ratio in the range of 0.25 to 0.5.

6- Lateral load on pile contributes by about 50% of induced B.M, about 17% of induced compression axial force and about 2% of induced tension axial force on tunnel lining.

7- Vertical load on pile causes about 95% of induced vertical deformation of tunnel lining, while nearly 100% of lateral deformation comes from lateral load on pile.

8- The weaker the soil, the most the effect of pile loading on the existing tunnel lining.

6. REFERENCES

[1] A. D. Withers, “37 Surface displacements at three surface reference sites above twin tunnels through the Lambeth Group,” in Building response to tunnelling: Case studies from construction of the Jubilee Line Extension, London, Thomas Telford Publishing, 2001, pp. 735–754.

[2] R. B. Peck, “Deep excavations and tunneling in soft ground,” Proc. 7th ICSMFE, 1969, pp. 225–290, 1969.

[3] P. B. Attewell, “Predicting the dynamics of ground settlement and its derivatives caused by tunnelling in soil,” Ground engineering, vol. 15, no. 8, pp. 13–22, 1982.

[4] N. Loganathan and H. G. Poulos, “Analytical prediction for tunneling-induced ground movements in clays,” Journal of Geotechnical and geoenvironmental engineering, vol. 124, no. 9, pp. 846–856, 1998.

[5] Pickhaver and John Anthony, “Numerical modelling of building response to tunnelling,” University of Oxford, 2006.

[6] A. D. Withers, “42 Murdoch, Neptune and Clegg Houses in Moodkee Street, Rotherhithe,” in Building response to tunnelling: case studies from construction of the Jubilee Line Extension, London, Thomas Telford Publishing, 2001, pp. 811–828.

[7] H. J. Burd, G. T. Houlsby, C. E. Augarde, and G. Liu, “Modelling tunnelling-induced settlement of masonry buildings,” Proceedings of the institution of civil engineers-geotechnical engineering, vol. 143, no. 1, pp. 17–29, 2000.

[8] J. A. Pickhaver, “Numerical modelling of building response to tunnelling.” University of Oxford Oxford, UK, 2006.

[9] A. M. Marshall and T. Haji, “An analytical study of tunnel–pile interaction,” Tunnelling and Underground Space Technology, vol. 45, pp. 43–51, 2015.

[10] M. A. Soomro, C. W. W. Ng, K. Liu, and N. A. Memon, “Pile responses to side-by-side twin tunnelling in stiff clay: Effects of different tunnel depths relative to pile,” Computers and Geotechnics, vol. 84, pp. 101–116, 2017.

[11] N. Heama, P. Jongpradist, P. Lueprasert, and S. Suwansawat, “Investigation on p ile- s oil-t unnel i nteraction d ue to a djacent l oaded p ile r ow by 3D FEM,” vol. 02051, pp. 1–4, 2018.

[12] C. Yoo, “Three dimensional numerical investigation on the effect of bridge construction on existing tunnel,” KSCE Journal of Civil Engineering, vol. 18, no. 3, pp. 794–802, 2014.

[13] S. C. Möller, Tunnel induced settlements and structural forces in linings. Univ. Stuttgart, Inst. f. Geotechnik Stuttgart, Germany, 2006.

[14] W. J. M. Rankine, “On the Stability of Loose Earth.,” Proceedings of the Royal Society of London, pp. 185–187, 1856.

[15] P. Bv, “PLAXIS 3D user manulas,” 2019.

[16] C. H. Pang, K. Y. Yong, Y. K. Chow, and J. Wang, “The response of pile foundations subjected to shield tunnelling,” 2006.

[17] British Standards Institution, The code of practice for site investigations. 1981.

[18] W. G. Zhang, R. H. Zhang, L. Han, and A. T. C. Goh, "Engineering properties of the Bukit Timah Granitic residual soil in Singapore," Underground Space, vol. 4, no. 2, pp. 98–108, 2019.

[19] K. D. Krank and R. J. Watters, "Geotechnical properties of weathered Sierra Nevada granodiorite," Bulletin of the Association of Engineering Geologists, vol. 20, no. 2, pp. 173–184, 1983.

[20] M. A. Adam, A. M. Elleboudy, and M. F. Soliman, "Seismic Site Response Analysis of a Cairo Metro Tunnel," Geotechnical and Structural Engineering Congress 2016 - Proceedings of the Joint Geotechnical and Structural Engineering Congress 2016, pp. 1114–1126, 2016, doi: 10.1061/9780784479742.093.

[21] ECP202, Egyptian code of practice for soil mechanics and foundations. 2001.